Fuzzy Homogeneity Measures for Path-based Colour Image Segmentation

J. Chamorro-Martínez, D. Sánchez, B. Prados-Suárez, E. Galán-Perales
Department of Computer Science and Artificial Intelligence, University of Granada
C/ Periodista Daniel Saucedo Aranda s/n, 18071 Granada, Spain
e-mail : {jesus,daniel,belenps,elena}@decsai.ugr.es

Abstract— **In this paper we study different measures of path homogeneity for fuzzy path-based image segmentation. We provide fuzzy semantics for the concept of homogeneity in two steps: first, we introduce a fuzzy interpretation of resemblance between feature vectors characterizing neighbor pixels; then, we obtain the homogeneity of a path by aggregating the set of fuzzy resemblances between consecutive pixels in the path. We propose a set of intuitive properties that any suitable aggregation function should verify for this purpose, and we show that these properties are verified by certain families of t-norms. To determine the performance of the proposed functions, a set of experiments is carried out with both synthetic and real images. Finally, the homogeneity functions are used to obtain fuzzy regions in natural images.**

Keywords: Image segmentation, fuzzy segmentation, path-based segmentation, fuzzy connectivity, fuzzy colour homogeneity.

I. Introduction

Image segmentation is defined as a partition of the image into connected subsets of pixels, called regions, on the basis of some homogeneity criterion. Usually, this is the starting point in a wide number of applications like image database retrieval or robot vision [1].

Many types of segmentation techniques have been proposed in the literature, for example those based on histogram analysis [2], clustering [3], split and merge [4], region growing [5] and edge based algorithms [6]. It is certain that most of the proposals falling in the aforementioned categories, provide a crisp segmentation of images, where each pixel has to belong to an unique region. However, separation between regions is usually imprecise in natural images, as occurs in shadows, brights and colour gradients, where crisp techniques are not often appropriate. To solve this problem, some approaches propose the definition of *region* as a fuzzy subset of pixels, in such a way that every pixel of the image has a membership degree to that region [7], [8].

The majority of the fuzzy techniques are based on fuzzy clustering, like C-means algorithms, which defines a set of centroids and compute the membership value for all the pixels in the image to each centroid [9], [10]. Another examples are those based on the definition of fuzzy histograms [11] or fuzzy rule-based systems [12]. Nevertheless, a drawback of most of these fuzzy approaches is that they don't take into account that a region must be topologically connected. As a consequence, pixels belonging to separate and different regions could be assigned to the same cluster.

To face up to above-mentioned problem, path-based techniques arise which incorporate spatial information related to adjacency between pixels. These approaches are based on the idea of fuzzy topology, introduced by Rosenfeld [13], and the use of fuzzy connectivity to measure the relationship between any pair of pixels. Thus, given a region representative point (called seed point), the path-based methods obtain the associated fuzzy region on the basis of the connectivity between the seed point and the rest of pixels in the image [5], [7], [14].

In the context of path-based image segmentation, an open problem is how to measure the homogeneity of a "path" connecting two pixels and, based on this measure, the membership degree of its fuzzy connectivity. Most of the approaches in the literature calculate heterogeneity from the set of distances between consecutive points in the path, being the most common solution the use of a simple aggregation function (sum or maximum) over this set of distances [5], [7], and finally obtaining homogeneity as a kind of inverse of heterogeneity. However, to our knowledge, there is not a study about the goodness of different homogeneity functions applied to image segmentation.

In this paper an experimental study of different aggregation functions to calculate homogeneity is performed. For this purpose, a set of desirable properties are defined and a set of candidates which verify these properties are proposed. To analyze the performance of the studied functions, a set of experiments is presented with synthetic and real images. Using the homogeneity functions analyzed in the experiment, the growing region algorithm proposed in [1] is used to obtain fuzzy regions by means of a fuzzy subset of connected pixels.

The rest of the paper is organized as follows: In section II we introduce the path-based segmentation techniques. Section III describes the desirable properties for the aggregation function and the candidates studied in this paper. Finally, the experimental results and the main conclusions are showed in sections IV and V respectively.

II. Path-based image segmentation

Path-based techniques incorporate spatial information related to adjacency between pixels (unlike the clustering-based methods, which classified each pixel without considering its neighborhood). In these approaches, the segmentation is performed by measuring the connectivity between any pair of pixels as the homogeneity degree of the most homogeneous path joining them [14]. In a fuzzy approach, given a set of seed points, fuzzy regions are obtained on the basis of the connectivity between each seed point and the rest of pixels in the image [14], [7].

In this section we present a path-based methodology to obtain image regions as fuzzy subsets of connected pixels. First, we need to fix the features that characterize a pixel. A fuzzy resemblance relation between neighbor pixels is obtained from a fuzzy resemblance relation between their corresponding feature vectors. This concept is extended later to any pair of pixels following the aforementioned path-based approach. The whole process is particularized for the case of colour features.

A. Pixel characterization

We characterize each pixel p by means of a vector of features $\overrightarrow{f_p}$

$$\overrightarrow{f_p} = \left[f_p^1, f_p^2, \dots, f_p^n\right] \tag{1}$$

where a feature $f_p^i \in \mathbb{R}$, with $i \in \{1, 2, \dots, n\}$, is a numerical measure of any relevant characteristic that may be obtained for p. As an example of feature vector, let's think about a three band colour representation like RGB.

In this work we are concerned with segmentation on the basis of colour, i.e., we want to obtain a set of homogeneously-coloured regions. Hence, we are interested in colour features.

1) Characterization by colour: Although the RGB is the most used model to acquire digital images, it is well known that it is not adequate for colour image segmentation. Instead, other colour spaces based on human perception (HSI, HSV or HLS) seem to be a better choice for this purpose [15]. In these spaces, hue (H) represents the colour tone (for example, red or blue), saturation (S) is the amount of colour (for example, bright red or pale red) and the third component (called intensity, value or lightness) is the amount of light (it allows the distinction between a dark colour and a light colour).

In this paper, the HSI colour space will be used (it offers many advantages in a segmentation process, for example, the use of hue avoids the shading effects). Geometrically, this colour space is represented as a cone, in which the axis of the cone is the grey scale progression from black to white, distance from the central axis is the saturation, and the direction is the hue (figure 1). To calculate the HSI values from the RGB coodinates, the following transform is applied [15]:

$$\begin{array}{l} H = \arctan\left(\frac{\sqrt{3}(G+B)}{2R-G-B}\right) \\ S = 1 - \min\{R, G, B\}/\, I \\ I = (R+G+B)/\,3 \end{array} \tag{2}$$

Therefore, in this paper a pixel p will be characterized using the three band colour representation given by the HSI colour space:

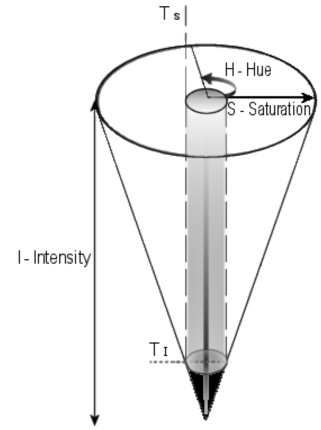

Fig. 1. HSI colour space

$$\overrightarrow{f_p} = [H_p, S_p, I_p] \tag{3}$$

B. Fuzzy Resemblance between feature vectors

In image segmentation, regions consist of a set of connected pixels whose features are resemblant, i.e., not different. Hence, we need to define resemblance between feature vectors, and a suitable tool for that purpose is the concept of fuzzy resemblance relation.

In general, we define a fuzzy resemblance relation between (real) feature vectors as a fuzzy subset $\mathcal{FR}$ of $\mathbb{R}^n \times \mathbb{R}^n$, with membership function

$$\mathcal{FR} : \mathbb{R}^n \times \mathbb{R}^n \to [0, 1]$$

verifying the reflexive and symmetric properties, i.e., given two feature vectors $\overrightarrow{f_1}$ and $\overrightarrow{f_2}$, $\mathcal{FR}(\overrightarrow{f_1}, \overrightarrow{f_1}) = 1$ and $\mathcal{FR}(\overrightarrow{f_1}, \overrightarrow{f_2}) = \mathcal{FR}(\overrightarrow{f_2}, \overrightarrow{f_1})$.

The way resemblance between feature vectors is computed depends on the concrete features employed. Usually, resemblance between particular features or subvectors is calculated, depending on the specific feature domain, and then the resulting measures are aggregated. Finally, differences between subvectors of features may be aggregated using some appropriate aggregation function.

1) Resemblance between colours: In this paper the resemblance between pixel features will be measured by means of the resemblance between colour features, which will be calculated on the basis of distances in the HSI colour space.

Distance between colours in the HSI space

The distance between two colour stimuli $c_1 = [H_1, S_1, I_1]$ and $c_2 = [H_2, S_2, I_2]$ can be defined on the basis of the differences between its components:

$$\begin{array}{l} \triangle_H(c_1, c_2) = \begin{cases} \frac{|H_1 - H_2|}{\pi} & if\, |H_1 - H_2| \leq \pi \\ \frac{2\pi - |H_1 - H_2|}{\pi} & otherwise \end{cases} \\ \triangle_S(c_1, c_2) = |S_1 - S_2| \\ \triangle_I(c_1, c_2) = \frac{|I_1 - I_2|}{MAXI} \end{array} \tag{4}$$

$$\triangle C(c_1, c_2) = \begin{cases} \triangle_I & if\ p_i\ or\ p_j\ are\ achromatic \\ \frac{1}{\sqrt{3}}\left[\triangle_I^2 + \triangle_S^2 + \triangle_H^2\right]^{1/2} & if\ p_i\ and\ p_j\ are\ chromatic \\ \frac{1}{\sqrt{2}}\left[{\triangle_I}^2 + {\triangle_S}^2\right]^{1/2} & otherwise \end{cases} \tag{5}$$

with $MAXI$ being a constant equals to the maximum level of intensity, usually 255 (let us remark that $\triangle_H, \triangle_S, \triangle_I \in [0, 1]$). Based on the previous distances, the equation 5 will be used to measure the difference between colours (for the sake of simplicity, we have removed the parameters (c_1, c_2) in the notation $\triangle_H$, $\triangle_S$ and $\triangle_I$). Notice that $\triangle C(c_1, c_2) \in [0, 1]$.

In equation 5 we introduce the notions of chromaticity/achromacitiy to manage two well known problems of the HSI representation: the imprecision of the hue when the intensity or the saturation are small, and the non-representativity of saturation under low levels of intensity. An often practical solution to solve this problem is to perform a partition of the colour space based on the chromaticity degree of each point. In equation (5), we propose to split the HSI space into three regions: *chromatic*, *semi-chromatic* and *achromatic* (figure 1) on the basis of thresholds T_I and T_S on the components I and S respectively. A color $c_i = [H_i, S_i, I_i]$ will be *achromatic* if $I_i \leq T_I$ (black zone in figure 1), *semi-chromatic* if $I_i > T_I$ and $S_i \leq T_S$ (grey zone in figure 1), and *chromatic* if $I_i > T_I$ and $S_i > T_S$ (white zone in figure 1). In this paper, the thresholds have been fixed empirically to $T_I = MAXI/5$ and $T_s = 1/5$.

Resemblance between colours in the HSI space

On the basis of the distance between colours given by the equation 5, we define the resemblance between the feature vectors f_p and f_q corresponding to pixels p and q of an image I as

$$\mathcal{FR}(\overrightarrow{f_p}, \overrightarrow{f_q}) = 1 - \frac{\triangle C(\overrightarrow{f_p}, \overrightarrow{f_q})}{M} \tag{6}$$

where $\overrightarrow{f_p} = [H_p, S_p, I_p]$ and $\overrightarrow{f_q} = [H_q, S_q, I_q]$ are the colour features vector of p and q respectively, and M is a normalization factor given by

$$M = \max\left\{\triangle C(\overrightarrow{f_r}, \overrightarrow{f_s})\ ,\ r\ and\ s\ \in I\right\} \tag{7}$$

A final comment concerns the choice of the normalization factor M. The two natural choices are i) to normalize with respect to the maximum difference between pixels in the image, and ii) to normalize with respect to the maximum difference in the feature domain. We have chosen the first option because it allows us to obtain more significant resemblance values in those images where only a small part of the feature vector space appears. This choice has lead us to obtain better results in practice.

The case $M = 0$, in which the resemblance is undefined, is not considered here because in that case the image is a set of pixels with exactly the same features, and hence the result of the segmentation is trivially one single region comprising the whole image.

C. *Fuzzy Connectivity between pixels*

In fuzzy path-based image segmentation, the notion of fuzzy connectivity of two pixels indicates to which degree those pixels belong to a group of topologically connected pixels with resemblant features. Because of this, to measure the fuzzy connectivity between two pixels we do not use directly the resemblance between their feature vectors, but we use information about the homogeneity of the paths joining them. Before entering into details, let us introduce some definitions:

Definition 2.1: A path between two pixels p and q is a sequence

$$\pi_{pq} = (r_1, r_2, \ldots, r_k) \tag{8}$$

where $k \geq 1$, such that $r_1 = p$ and $r_k = q$ and r_i is connected to r_{i+1} $\forall i \in \{1, \ldots, k-1\}$

We note $\prod_{pq}$ the set of possible paths linking the pixels p and q through pixels of the image I. Also, we note $\mathcal{P}(\pi_{pq})$ the set of pixels in the path π_{pq}, and π_{pq}^{rs} the subpath of π_{pq} that connects r and s with $r, s \in \mathcal{P}(\pi_{pq})$, and r appearing before s. Also, let $\pi_{pq} = \{p_1, \ldots, p_n\}$, then $\pi_{pq}^{-1} = p_n, \ldots, p_1$.

Definition 2.2: The fuzzy homogeneity of a path $\pi_{pq} \in \prod_{pq}$, is defined as a function

$$homo : \Pi_{pq} \rightarrow [0, 1] \tag{9}$$

calculated on the basis of the resemblances between consecutive points on the path.

To measure the resemblances between consecutive points, the relation $\mathcal{FR}$ will be used. In section III we shall study desirable properties of $homo$ and we shall propose some candidate functions.

Taking into account the $homo$ function, we define the optimum path between p and q, $\hat{\pi}_{pq}$, as the path that links both points with maximum homogeneity, in the following way:

Definition 2.3: The optimum path between p and q is:

$$\hat{\pi}_{pq} = \underset{\pi_{pq} \in \Pi_{pq}}{argmax} \quad \{homo(\pi_{pq})\} \tag{10}$$

Based on this optimum path, we can get the measure of the connectivity between two pixels as follows:

Definition 2.4: The fuzzy connectivity between two pixels p and q is the homogeneity of the optimum path from p to q:

$$conn(p, q) = homo(\hat{\pi}_{pq}) \tag{11}$$

Let us remark that the homogeneity measure defined in (11) uses topographic information (paths linking the pixels) and resemblance between pixel features.

D. Membership function for fuzzy regions

In the above section we have introduced the use of paths to measure the fuzzy connectivity between any pair of pixels. Now this connectivity will be used to obtain fuzzy regions in an image I by means of the growing region algorithm proposed in [1]. Concretely, in this approach a region is defined as a fuzzy subset of connected pixels, so it is necessary to define a measure that indicates the degree in which each pixel in the image I belongs to each region. Under the assumption that a fuzzy region $\widetilde{R_s}$ has a representative seed point r_s (as in the region growing techniques), we introduce the following membership function associated to each region:

Definition 2.5: The membership degree $\mu_{\widetilde{R_s}}(p)$ of a pixel p in a fuzzy region $\widetilde{R_s}$ is defined as:

$$\mu_{\widetilde{R_s}}(p) = conn(p, r_s) \tag{12}$$

where r_s is the seed point of $\widetilde{R_s}$

Using equation (12) we can calculate the membership degree of every point $p \in I$ to each region $\widetilde{R_s}$. This allows us to obtain a set of fuzzy regions $\widetilde{\Theta} = \left\{\widetilde{R}_1, \widetilde{R}_2, \ldots, \widetilde{R}_m\right\}$ from a set of seed points $\Theta = \{r_1, r_2, \ldots, r_m\}$. An algorithm to calculate $\widetilde{\Theta}$ is proposed in [1] with a computational complexity of $O(mn)$, where n is the number of pixels and m is the number of seeds.

III. Measuring the homogeneity of a path

In previous section we have described a methodology for path-based fuzzy segmentation. In this section we discuss about possible ways to measure the homogeneity of a path.

A. Path Homogeneity Intuition

Let $\pi_{pq} = r_1 \ldots r_n$ be a path. We want to come up with a function $homo(\pi_{pq})$ measuring the homogeneity of the path π_{pq}. For the sake of simplicity, let us define a resemblance relation $\mathcal{PR}$ between neighbor pixels, induced by the relation $\mathcal{FR}$ between their corresponding features, in the following way:

$$\mathcal{PR}(p, q) = \mathcal{FR}(\overrightarrow{f_p}, \overrightarrow{f_q})$$

Hence, it seems natural to define $homo(\pi_{pq})$ as an aggregation of the resemblances between consecutive points in the path π_{pq}, i.e., $homo(\pi_{pq}) = Aggr(ReSet(\pi_{pq}))$, where $ReSet$ is the following bag (multiset) of values:

$$ReSet(\pi_{pq}) = \{\mathcal{PR}(r_k, r_{k+1}) \mid r_k, r_{k+1} \in \mathcal{P}(\pi_{pq})\}$$

In order to choose the aggregation function $Aggr$, we study first the set of properties that the $homo$ function should verify. We propose the following minimal set of properties for $homo$:

1) Let $\pi_{pq} = p, q$ be a path consisting of two adjacent pixels. Then $homo(\pi_{pq}) = \mathcal{PR}(p, q)$. As a consequence, if $\pi_{pp} = p, p$ then $homo(\pi_{pp}) = 1$.
2) The homogeneity of a path should be less or equal that the resemblance between consecutive pixels in the path, i.e., $homo(\pi_{pq}) \leq \min ReSet(\pi_{pq})$. The rationale behind this property is that a path is completely homogeneous if *all* the possible pairs of consecutive pixels are resemblant. Hence, the homogeneity of the path has an upper bound in the minimum value of resemblance between pairs of consecutive pixels.
3) Monotony: $homo(\pi_{pq}^{rs}) \geq homo(\pi_{pq})$.
4) Let π_{pq} and $\pi_{p'q'}$ be two paths such that $ReSet(\pi_{pq}) = ReSet(\pi_{p'q'})$. Then $homo(\pi_{pq}) = homo(\pi_{p'q'})$. In particular, $homo(\pi_{pq}) = homo(\pi_{pq}^{-1})$.

These properties suggest to use a t-norm to aggregate the resemblances between consecutive pixels into the final homogeneity of the whole path, i.e., to define the aggregation function as

$$Aggr(ReSet(\pi_{pq})) = \bigwedge ReSet(\pi_{pq}) \tag{13}$$

were $\wedge$ is a t-norm.

It is trivial to show that this function satisfy all the properties we have required.

B. Some candidates

The choice of the t-norm to be used in equation 13 depends on the application at hand. In order to discuss about this issue we have performed some experiments, where we have employed the following operators:

- Minimum
- Algebraic product $I_A(a, b) = ab$.
- Bounded difference $I_B(a, b) = \max(0, a + b - 1)$.
- Dubois-Prade's parametric t-norm:

$$I_{DP}(a, b) = \frac{ab}{\max(a, b, \alpha)} \tag{14}$$

  with $\alpha \in [0, 1]$.
- Weber's parametric t-norm:

$$I_W(a, b) = \max\left(0, \frac{a + b + \lambda ab - 1}{1 + \lambda}\right) \tag{15}$$

  with $\lambda > -1$.
- Frank's parametric t-norm:

$$I_F(a, b) = \log_s\left(1 + \frac{(s^a - 1)(s^b - 1)}{s - 1}\right) \tag{16}$$

  with $s > 0$, $s \neq 1$.

We have chosen the last three operators (Dubois-Prade's, Weber's and Frank's parametric t-norms) because:

- They are parametric, so we can study different aggregation alternatives by using different parameters of these well known operators.
- We consider that in most of the cases, t-norms that yield values under those provided by the bounded difference are too strict because the resulting homogeneity values are too low in general, and hence significant membership values of fuzzy regions tends to be too low. Hence, we have chosen parametric operators that yield values between the minimum and the bounded difference.

We have considered the first three t-norms, though they are known to be particular cases of the other three, as they are very well known, as well as their properties. In the next section we show some results and we discuss about using these t-norms, with several parameters, to calculate the homogeneity of a path.

IV. Experimental results

A. Synthetic images

To test the behavior of the aforementioned t-norms we have used synthetic images simulating different shades. One of them, that serves to summarize our conclusions, is shown in figure 2, where we have an image of size 256x256 showing a red toning down computed by means of a gaussian function applied on the saturation component.

The graphical representations in figures 2-A1 to 2-A3 show evolution of the homogeneity degree along the path indicated by a black line in figure 2, computed with different aggregation functions. Specifically, for each $i \in \{1, \ldots, 255\}$ in the X axis, the graphics show in the Y axis the homogeneity degree of the subpath from (0,0) to (i,i).

Two main behaviors have been found among these t-norms. On the one hand, we have functions with big slopes that reach the minimum homogeneity value in a point of the path close to the seed of the region. It means that all the pixels after this one have minimum membership degree, so the influence area of the region will be small. It produces regions where the fade is fast at each bound, useful in images where it is necessary to find a frontier between regions whose bounds are fuzzy. This is the case of Weber t-norm when its parameter takes values under approximately -0.35.

On the other hand, small slopes implies small and similar homogeneity values, so minimum homogeneity will only be reached in a pixel very far away from the origin of the region. The limit case is given by functions like minimum or Dubois-Prade t-norm with parameter under 0.997, that have a point from which they are constant, so never reach minimum homogeneity). At the same time, homogeneity takes values in just a small part (the upper one) of the theoretical range. This kind of functions may be used, for example, in homogeneous but noisy images, where we want to overcome noise influence, or in images where we want to let regions spread without any limit.

Finally, between both extreme behaviors there is a wide range of functions like for example Frank's t-norm, whose homogeneity curves for this example are showed in figure 2-A3. In this case, when the parameter s increase, the function assigns higher homogeneity values to pixels in the path and capture lower decreasing shades. Difference between the graphics of consecutive functions is smaller as s grows.

B. Real images

In these section we will show an example of the usefulness of this variety of behaviors, applied to a real image shown in figure 3. In this experiment we have placed one seed in the

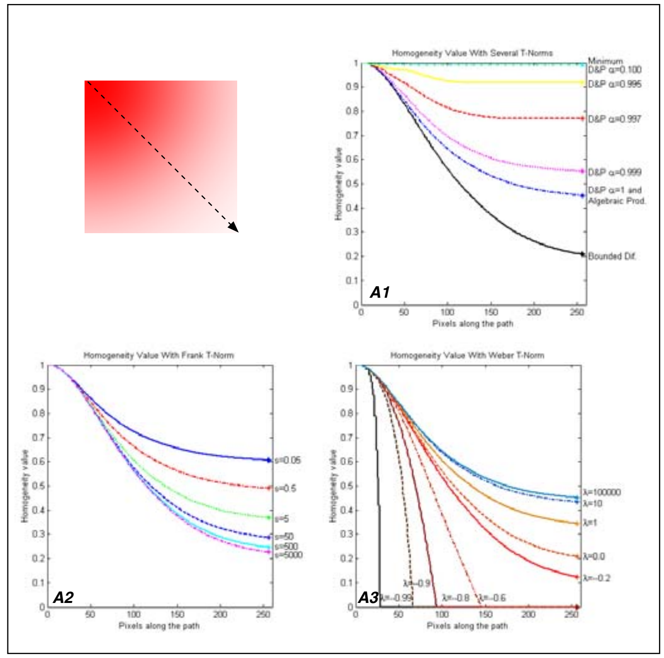

Fig. 2. *Results with a synthetic image generated by means of a Gaussian function simulating a toning down from a light incidence point.*

image, and we have computed the corresponding fuzzy region using different t-norms.

In all the cases, the first and second columns represent the membership value to a given seed, computed with a certain cost function. In the first column, membership degrees are represented as gray levels; white colour means maximum membership value while black is the minimum. In the second one, a 3D representation of the region is shown, where the height of a point is its membership degree. The last column shows the area corresponding to a certain α-cut of the fuzzy region. Rows A, B and C correspond to the results obtained using Dubois-Prade t-norm with $s = 0.997$, Frank's with $s = 50$, and Weber's with $\lambda = -0.8$, respectively.

In images 3-A1 to C1, we can see that the higher membership degrees correspond to the red round pepper, and how there is a significant decrease of membership degrees out of the boundary of the pepper, as expected. The magnitude of that decrease, that depends on the t-norm employed, as we discussed in the experiment with synthetic images, can be better appreciated in the second column of images. We can see how in figure C1, almost the rest of the image takes value 0 of membership, limiting the extent of the region to almost just the red round pepper. This is shown also in image C2. In the other two cases, the support of the fuzzy region is almost the whole image.

In all the cases, it is possible to find an α-cut which bounds rather well the area of the pepper. The figures in the third column show these α-cuts with values α of ≈ 0.77, ≈ 0.62, and ≈ 0.73, respectively.

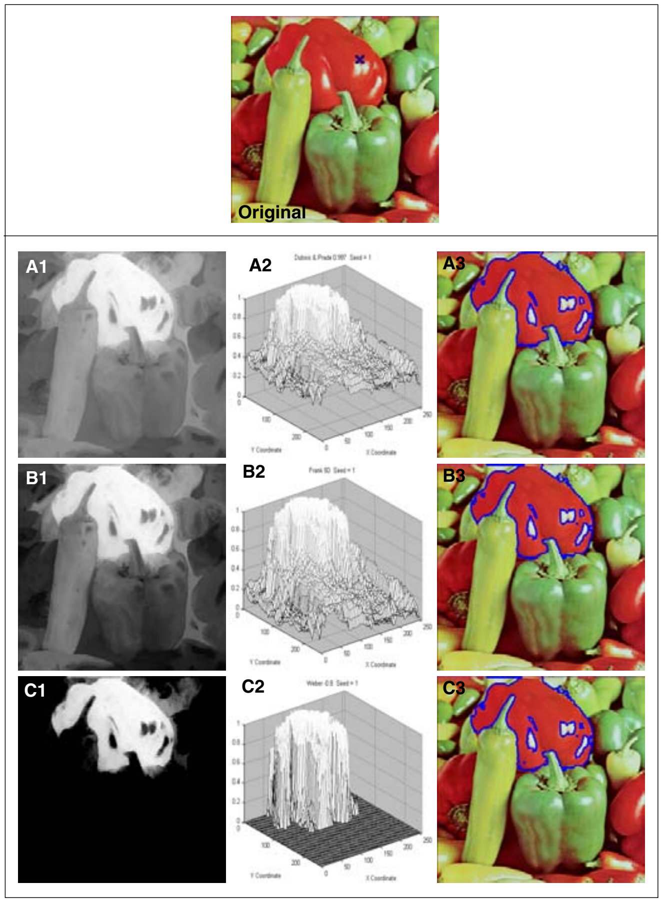

Fig. 3. Results with a real image

V. Conclusions

Path-based fuzzy image segmentation takes a colour image and yields a set of fuzzy regions, each region being a fuzzy subset of topologically connected pixels. As a way to determine membership degrees, we have proposed a fuzzy approach to calculate the homogeneity of a path. The homogeneity degree of a path is obtained as an aggregation of resemblances between colours of adjacent pixels in the path. Starting from a set of intuitive properties, we have chosen to employ t-norms as aggregation operators.

We have studied the use of different t-norms that present a wide range of behaviors, giving us a powerful and flexible tool to adapt membership functions of fuzzy regions to any kind of colour image, depending on its purpose and characteristics.

Summarizing, two main different behaviors of t-norms have been found. On the one hand, we have functions with steep slopes like Weber's functions with $\lambda \in (-1, 0.5]$, that are the most suitable ones when we are looking for homogeneous regions with relatively small imprecise bounds (for example, unicellular organisms in biomedical images). On the other hand, functions with soft slopes like bounded difference or algebraic product are useful when most of the region is imprecise and there is not a clear region bound (for example, nebula images in astronomy, intercellular material in biomedical images, or toning down images like that in figure 2). In general, from the order relation existing between t-norms, from minimum to the bounded difference, we obtain different slopes for the membership functions, allowing us to move from obtaining relatively small and clearly differentiated regions (due to a fast decreasing in homogeneity as we move away from the seed) to larger regions with more imprecise boundaries (if the decreasing is softer). The experiments we have performed show this behavior. In particular, it can be appreciated that the results are coherent with what we could expect as a result of the segmentation process.

As future work we shall study an automatic procedure to select the most suitable function depending on the characteristics of the regions in the image.

References

[1] J. Chamorro-Martinez, D. Sanchez, and B. Prados-Suarez, *A Fuzzy Color Image Segmentation Applied to Robot Vision*. In Advances in Soft Computing - Engineering, Design and Manufacturing. J.M. Benitez, O. Cordon, F. Hoffman, and R. Roy (ed.). Springer., 2003, pp. 129–138.

[2] A. Gillet, L. Macaire, C. Botte-Lococq, and J. Postaire, "Color image segmentation by fuzzy morphological transformation of the 3d color histogram," *Proceedings of the 10th IEEE International Conference on Fuzzy Systems*, vol. 2, pp. 824 –824, 2001.

[3] D. Zhong and H. Yan, "Color image segmentation using color space analysis and fuzzy clustering," *Proceedings of the 2000 IEEE Signal Processing Society Workshop*, vol. 2, pp. 624– 633, 2000.

[4] G. Borges and M. Aldon, "A split-and-merge segmentation algorithm for line extraction in 2d range images," *Proceedings of the 15th International Conference on Pattern Recognition*, vol. 1, pp. 441 – 444, 2000.

[5] A. Moghaddamzadeh and N. Bourbakis, "A fuzzy region growing approach for segmentation of color images," *Pattern Recognition*, vol. 30, no. 6, pp. 867–881, 1997.

[6] A. Shiji and N. Hamada, "Color image segmentation method using watershed algorithm and contour information," *Proceedings of International Conference on Image Processing*, vol. 4, pp. 305 – 309, 1999.

[7] B. Cavalho, C. Gau, G. Herman, and T. Kong, "Algorithms for fuzzy segmentation," *Proceedings of the International Conference on Advances in Pattern Recognition*, pp. 154–63, 1999.

[8] J. Chamorro-Martinez, D. Sanchez, B. Prados-Suarez, E. Galan-Perales, and M. Vila, "A hierarchical approach to fuzzy segmentation of colour images," in *IEEE International Conference on Fuzzy Systems*, vol. 2. St. Louis, Missouri (USA), May 2003, pp. 966–971.

[9] J.-F. Yang, S.-S. Hao, and P.-C. Chung, "Color image segmentation using fuzzy c-means and eigenspace projections," *Signal Processing*, vol. 82, pp. 461–472, 2002.

[10] Y. Zhao and M. Li, "A modified fuzzy c-means algorithm for segmentation of mri," *Proceedings of the fifth International Conference on Computational Intelligence and Multimedia Applications (ICCIMA 2003), 27-30 September*, pp. 391–395, 2003.

[11] J. Han and K.-K. Ma, "Fuzzy color histogram and its use in color image retrieval," *IEEE Transactions on Image Processing*, vol. 11, no. 8, pp. 944–952, 2002.

[12] F. Hacbouf and N. Mezhoud, "An improved fuzzy rule-based segmentation system," *Proceedings of the Seventh International Symposium on Signal Processing and Its Applications, July 1-4 2003*, vol. 1, pp. 533–536, 2003.

[13] A. Rosenfeld, "Fuzzy digital topology," *Information and Control*, vol. 40, no. 1, pp. 76–87, 1979.

[14] J. Udupa and S. Samarasekera, "Fuzzy connectedness and object definition: Theory, algorithms and applications in image segmentation," *Graphical Models and Image Processing*, vol. 58, no. 3, pp. 246–261, 1996.

[15] J. Russ, *The Image Processing Handbook*, 3rd ed. CRC Press and IEEE Press, 1999.